

# A Conservative Finite Element Method for One-Dimensional Stefan Problems with Appearing and Disappearing Phases

R. BONNEROT AND P. JAMET

*Commissariat à l'Energie Atomique, Centre d'Etudes de Limeil,  
Service de Mathématiques Appliquées, B.P. 27, 94190, Villeneuve Saint-Georges, France*

Received May 28, 1980

A one-dimensional Stefan problem involving several phases (solid, liquid, vapor) which can appear and disappear is considered. A numerical method for such problems is described and numerically tested. It is derived from a previous method of the same authors for one-phase problems. It is a front-tracking method based on finite elements in space and time. The treatment of the boundary conditions and the computation of the moving boundaries guarantee the exact conservation of heat energy. The numerical experiments demonstrate the accuracy and efficiency of the method. Moreover, they show that the appearing interfaces start smoothly with a vanishing initial speed; to the authors' knowledge, this property has not been mathematically proved.

## 1. INTRODUCTION

Many numerical methods are available for solving Stefan problems (see the references contained in [6, 9, 10, 12, 13]). Front-tracking methods can provide a better accuracy than methods which avoid the explicit computation of the front; but they have been applied only to relatively simple cases. In this paper, we consider a one-dimensional multiphase Stefan problem involving the appearance and disappearance of certain phases. In order to solve such problems with great accuracy, we extend and modify the third order accurate front-tracking method of [1]. The extensions concern the nature of the boundary conditions, the existence of several phases and the fact that the phases can appear and disappear. The modification concerns the treatment of the boundary conditions in order to make the scheme conservative.

We give a complete description of this revised method. It is based on finite elements in space and time. The position of the moving boundaries and the times of appearance and disappearance of each phase are explicitly computed. At each time step, the approximations are discontinuous and the finite elements can be arbitrarily chosen. A curved triangular element is used for each appearing or disappearing phase, while curved trapezoidal elements are used elsewhere. In each phase and at each time step, the number of finite elements is chosen according to the size of the

corresponding domain: it increases for an expanding phase and decreases for a shrinking phase, so that all elements have approximately the same size throughout the computation.

Numerical experiments are described for two cases of a multiphase Stefan problem. The results obtained for different choices of the "mesh-size" are presented in tables. The comparison of these results show that the temperature, the times of appearance and disappearance of each phase and the position of the moving boundaries are easily computed with a relative error of the order of  $10^{-5}$ : in the first case, which involves two moving boundaries, it is sufficient to take approximately 20 elements in the average at each time step; in the second case, which involves only one moving boundary, it is sufficient to take approximately 10 elements at each time step. For each of these problems, we have also studied the speed of propagation of the moving boundaries especially near the time of their appearance: the numerical results show that the moving boundaries start smoothly with an initial speed equal to zero. To the authors' knowledge, a rigorous proof of this property has not yet been given. (See [2, 3, 11] for mathematical results concerning the appearance and disappearance of phases.)

The plan of this paper is the following. In Section 2, we describe the problem that we want to solve. In Section 3, we give the principle of our Galerkin-type numerical method. In Section 4, we give the details concerning the use of finite elements. Finally, Section 5 is devoted to the numerical experiments.

## 2. A MULTIPHASE STEFAN PROBLEM

In this section, we introduce the problem that we want to solve. We first give a physical description of this problem. Then, we give a mathematical formulation. Finally, we derive an integral relation which admits the classical law of energy conservation as a particular case.

### 2.1. *Physical Description of the Problem*

We consider an infinite wall, i.e., a solid material which fills the region  $0 < x < a$ , where  $x$  is the space coordinate in the direction perpendicular to the wall and  $a$  is the thickness of the wall. We assume that the problem has slab symmetry; i.e., all the functions that we consider depend only on  $x$  and  $t$ , where  $t$  is the time variable.

The temperature of the wall at the initial time  $t = 0$  is given. Then, the wall is heated from the right by means of a given heat flux which is imposed on the right side of the wall ( $x = a$ ). The left side of the wall is thermally isolated; i.e., the heat flux is equal to zero for  $x = 0$ . The following phenomena take place.

#### *Appearance of a Liquid Phase (time $t = t_m$ )*

When the temperature on the right side of the wall reaches the melting temperature of the solid, a liquid phase appears. Assuming that the density of the liquid is equal

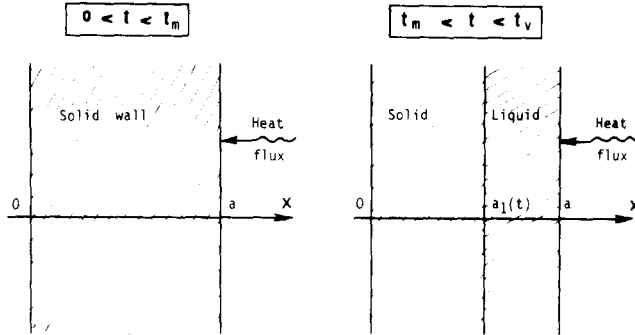


FIG. 1. The wall before and after the appearance of the liquid phase.

to the density of the solid, there is no displacement of the material: the solid lies in the region  $0 < x < a_1(t)$  and the liquid lies in the region  $a_1(t) < x < a$ , where  $x = a_1(t)$  is the position of the interface (see Fig. 1). The interface moves to the left and the temperature increases at any fixed point.

*Vaporization of the Liquid and Disappearance of the Solid Phase*

There are two possible cases.

*Case 1 (vaporization).* At a time  $t = t_v$ , before the complete melting of the solid, the temperature of the liquid on the right boundary ( $x = a$ ) reaches the vaporization temperature. Then, the liquid is vaporized on the right side and there appears an interface  $x = a_2(t)$  which separates the liquid from the gas. Assuming that the gas is removed as soon as it appears, there remains only two phases: the solid which lies in the region  $0 < x < a_1(t)$  and the liquid which lies in the region  $a_1(t) < x < a_2(t) < a$ . (See Fig. 2).

Ultimately, the interface  $x = a_1(t)$  reaches the left side of the wall ( $x = 0$ ); then, the solid phase disappears and the wall collapses (time  $t = t_f = \text{final time}$ ).

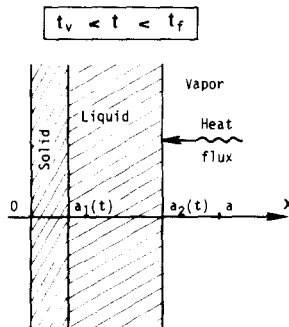


FIG. 2. The wall after the appearance of the vapor (Case 1).

*Case 2 (no vaporization).* When the interface  $x = a_1(t)$  reaches the left side of the wall, the temperature on the right side of the liquid has not yet reached the vaporization temperature. The solid phase disappears (time  $t = t_f$ ) before vaporization occurs.

## 2.2. Mathematical Description of the Problem

We will describe the problem in the case when vaporization occurs (Case 1). The other case is simpler and follows directly from Case 1 by removing the liquid-vapor interface.

We use the following notation.

The indices 1 and 2 correspond to the solid and liquid phases, respectively.  $u$  denotes the temperature.

*Independent variables:*  $x, t$ .

*Data:*

$u_m$  = melting temperature.

$u_v$  = vaporization temperature,  $u_m < u_v$ .

$\{a, c_1, c_2, K_1, K_2, C_m, C_v\}$  = set of positive constants.

$F(t)$  = positive function defined for  $t > 0$ .

$u^0(x)$  = function defined for  $0 \leq x \leq a$ , such that  $u^0(x) \leq u_m$  for all  $x$ .

The physical significance of these data is the following:  $c$  = heat capacity per unit volume,  $K$  = heat conductivity,  $C_m$  = latent heat of fusion per unit volume,  $C_v$  = latent heat of vaporization per unit volume,  $F(t)$  = heat flux on the right side of the wall,  $u^0(x)$  = initial temperature distribution.

*Unknowns:* (i)  $\{t_m, t_v, t_f\}$  = three values of the time,  $0 \leq t_m < t_v < t_f$ .

(ii)  $\{a_1(t), a_2(t)\}$  = two continuous functions defined for  $t_m \leq t \leq t_f$  and for  $t_v \leq t \leq t_f$ , respectively, and which satisfy the conditions

$$0 < a_1(t) < a, \quad \text{for } t_m < t < t_f,$$

$$0 < a_1(t) < a_2(t) < a, \quad \text{for } t_v < t < t_f,$$

$$a_1(t_m) = a_2(t_v) = a, \quad a_1(t_f) = 0.$$

(iii)  $u(x, t)$  = continuous function defined for  $0 \leq x \leq a$ ,  $0 \leq t \leq t_v$  and for  $0 \leq x \leq a_2(t)$ ,  $t_v \leq t \leq t_f$  and continuously differentiable in each of the two following domains:

$$\mathcal{R}_1 = \{(x, t); 0 < x < a, 0 < t \leq t_m\}$$

$$\cup \{(x, t); 0 < x < a_1(t), t_m < t < t_f\},$$

$$\mathcal{R}_2 = \{(x, t); a_1(t) < x < a, t_m < t \leq t_v\}$$

$$\cup \{(x, t); a_1(t) < x < a_2(t), t_v < t < t_f\}.$$

(See Fig. 3.)

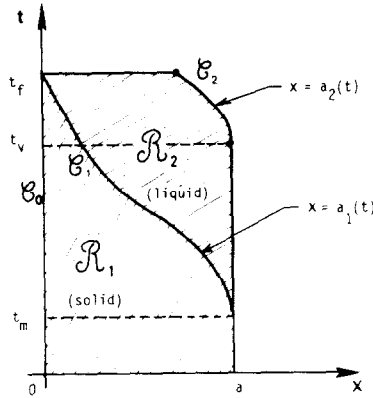


FIG. 3. The domain of definition of the function  $u$ .

We will denote by  $\mathcal{C}_0, \mathcal{C}_1$  and  $\mathcal{C}_2$  the curves defined by  $x=0, x=a_1(t)$  and  $x=a_2(t)$ , respectively. We will also use the notation

$$\left(\frac{\partial u}{\partial x}\right)_j = \text{the derivative } \frac{\partial u}{\partial x} \text{ in } \mathcal{R}_j, \quad j = 1 \text{ or } 2.$$

This distinction is essential at a point located on the interface  $\mathcal{C}_1$ . At other points, it is useless and may be omitted.

With these notations, the equations of the problem are the following.

*Partial differential equation for  $u(u, t)$ .*

$$c_j \frac{\partial u}{\partial t} - K_j \frac{\partial^2 u}{\partial x^2} = 0 \quad \text{in } \mathcal{R}_j, \quad j = 1 \text{ and } 2. \tag{2.1}$$

*Initial condition.*

$$u(x, 0) = u^0(x), \quad \text{for } 0 < x < a. \tag{2.2}$$

*Boundary conditions.*

$$\frac{\partial u}{\partial x} = 0 \quad \text{on } \mathcal{C}_0. \tag{2.3}$$

$$K_1 \frac{\partial u}{\partial x} = F(t), \quad \text{for } x = a, 0 < t < t_m. \tag{2.4}$$

$$K_2 \frac{\partial u}{\partial x} = F(t), \quad \text{for } x = a, t_m < t < t_v. \tag{2.5}$$

$$u = u_m \quad \text{on } \mathcal{C}_1. \tag{2.6}$$

$$u = u_v \quad \text{on } \mathcal{C}_2. \tag{2.7}$$

Differential equations for  $a_1(t)$  and  $a_2(t)$ .

$$C_m \frac{da_1}{dt} = K_1 \left( \frac{\partial u}{\partial x} \right)_1 - K_2 \left( \frac{\partial u}{\partial x} \right)_2 \quad \text{on } \mathcal{E}_1. \quad (2.8)$$

$$C_v \frac{da_2}{dt} = K_2 \left( \frac{\partial u}{\partial x} \right)_2 - F(t) \quad \text{on } \mathcal{E}_2.$$

Initial conditions for  $a_1(t)$  and  $a_2(t)$ .

$$a_1(t_m) = a_2(t_v) = a.$$

Conditions for  $t_m, t_v, t_f$ .

$$u(a, t_m) = u_m, \quad u(a, t_v) = u_v, \quad a_1(t_f) = 0.$$

*Remark.* If we assume that the solution  $u$  is such that each function  $(\partial u / \partial x)_1$  and  $(\partial u / \partial x)_2$  is continuous at the points which correspond to the appearance of a phase, it follows from (2.4), (2.5), (2.8) and (2.9) that

$$\begin{aligned} da_1/dt &= 0, & \text{for } t &= t_m, \\ da_2/dt &= 0, & \text{for } t &= t_v; \end{aligned} \quad (2.10)$$

i.e., each interface starts with a speed equal to zero. This is not a mathematical proof since the continuity of  $(\partial u / \partial x)_1$  and  $(\partial u / \partial x)_2$  should be proved.

We will see that relations (2.10) are in accordance with the numerical results.

### 2.3. Relation of Conservation

Let  $u$  be a function which satisfies

$$c \frac{\partial u}{\partial t} - K \frac{\partial^2 u}{\partial x^2} = 0 \quad \text{in a region } \mathcal{R}.$$

Let  $G$  be an arbitrary subdomain of  $\mathcal{R}$  and let  $\partial G$  be the boundary of  $G$  counter-clockwise oriented.

Let  $\Phi(G) = \text{Lip } \bar{G}$  = the set of all Lipschitz-continuous functions defined on the closure of  $G$  and let us assume  $u \in \Phi(G)$ .

Then, a classical integration by parts yields

$$\begin{aligned} & - \iint_G cu \frac{\partial \varphi}{\partial t} dx dt + \iint_G K \frac{\partial u}{\partial x} \frac{\partial \varphi}{\partial x} dx dt \\ & - \int_{\partial G} \varphi \left( cu dx + K \frac{\partial u}{\partial x} dt \right) = 0, \quad \text{for all } \varphi \in \Phi(G). \end{aligned} \quad (2.11)$$

In particular, for  $\varphi = 1$ , we get the relation of conservation:

$$-\int_{\partial G} \left( c u dx + K \frac{\partial u}{\partial x} dt \right) = 0. \tag{2.12}$$

We will apply this relation to the multiphase problem of Section 2.2.

Let  $\tau$  and  $\tau'$  be two values of  $t$  such that  $0 \leq \tau < \tau'$ . Let us assume that the two moving boundaries  $\mathcal{C}_1$  and  $\mathcal{C}_2$  exist at the times  $\tau$  and  $\tau'$ , i.e.,  $t_0 \leq \tau < \tau' \leq t_f$ , which is the more complicated case. Let  $G_1, G_2, \Gamma_0, \Gamma_1$  and  $\Gamma_2$  be the intersections of  $\mathcal{R}_1, \mathcal{R}_2, \mathcal{C}_0, \mathcal{C}_1$  and  $\mathcal{C}_2$  respectively, with the strip  $\tau < t < \tau'$ . Let  $\Omega_j$  and  $\Omega'_j$  be the intersections of  $\mathcal{R}_j$  with the lines  $t = \tau$  and  $t = \tau'$ , respectively, for  $j = 1$  and  $2$ . Let  $\Gamma_0, \Gamma_1, \Gamma_2$  be oriented towards increasing values of  $t$  and  $\Omega_1, \Omega_2, \Omega'_1, \Omega'_2$  be oriented towards increasing values of  $x$  (see Fig. 4).

The application of (2.12) to each of the domains  $G_1$  and  $G_2$  gives

$$\begin{aligned} & \int_{\Omega'_j} c_j u dx - \int_{\Omega_j} c_j u dx + \int_{\Gamma_{j-1}} c_j u dx - \int_{\Gamma_j} c_j u dx \\ & + \int_{\Gamma_{j-1}} K_j \frac{\partial u}{\partial x} dt - \int_{\Gamma_j} K_j \frac{\partial u}{\partial x} dt = 0, \quad \text{for } j = 1 \text{ and } 2. \end{aligned} \tag{2.13}$$

On the other hand, the integration of (2.8) and (2.9) between the times  $\tau$  and  $\tau'$  gives

$$\int_{\Gamma_1} K_1 \left( \frac{\partial u}{\partial x} \right)_1 dt - \int_{\Gamma_1} K_2 \left( \frac{\partial u}{\partial x} \right)_2 dt = C_m \Delta a_1, \tag{2.14}$$

$$\int_{\Gamma_2} K_2 \left( \frac{\partial u}{\partial x} \right)_2 dt = \int_{\tau}^{\tau'} F(t) dt + C_v \Delta a_2, \tag{2.15}$$

with  $\Delta a_j = a_j(\tau') - a_j(\tau)$ ,  $j = 1$  or  $2$ . Adding the two relations (2.13) corresponding to  $j = 1$  and  $2$  and taking (2.14) and (2.15) into account, we get

$$\begin{aligned} & \sum_{j=1}^2 c_j \left[ \int_{\Omega'_j} u dx - \int_{\Omega_j} u dx + \int_{\Gamma_{j-1}} u dx - \int_{\Gamma_j} u dx \right] \\ & + K_1 \int_{\Gamma_0} \frac{\partial u}{\partial x} dt - C_m \Delta a_1 - C_v \Delta a_2 = \int_{\tau}^{\tau'} F(t) dt. \end{aligned} \tag{2.16}$$

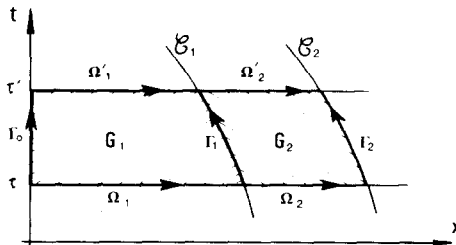


FIG. 4. The subdomains  $G_1$  and  $G_2$  and the oriented portions of their boundaries.

But,  $\partial u/\partial x = 0$  and  $dx = 0$  on  $\Gamma_0$ ,  $u = u_m$  on  $\Gamma_1$  and  $u = u_v$  on  $\Gamma_2$  (Eqs. (2.3), (2.6) and (2.7)). Finally, the relation of conservation can be written in the form

$$E_1 + E_2 + E_3 + E_4 + E_5 = E_6, \quad (2.17)$$

with

$$\begin{aligned} E_1 &= c_1 \left[ \int_{\Omega'_1} u \, dx - \int_{\Omega_1} u \, dx - u_m \Delta a_1 \right] \\ E_2 &= c_2 \left[ \int_{\Omega'_2} u \, dx - \int_{\Omega_2} u \, dx + u_m \Delta a_1 - u_v \Delta a_2 \right] \\ E_3 &= -C_m \Delta a_1, \quad E_4 = -C_v \Delta a_2, \\ E_5 &= \int_{\Gamma_0} K_1 \frac{\partial u}{\partial x} dt = 0, \quad E_6 = \int_{\tau}^{\tau'} F(t) dt. \end{aligned}$$

The physical significance of these terms is the following.

- $E_1$  = Energy used to heat the solid.
- $E_2$  = Energy used to heat the liquid.
- $E_3$  = Energy used to melt the solid.
- $E_4$  = Energy used to vaporize the liquid.
- $E_5$  = Loss of energy on the left boundary.
- $E_6$  = Energy provided on the right boundary.

The way in which we have derived the classical relation of conservation (2.17) from the integral relation (2.11) will be useful for finding a conservative numerical scheme, i.e., a scheme which yields approximations which satisfy the relation of conservation (2.17) exactly.

### 3. GENERAL DESCRIPTION OF THE NUMERICAL METHOD

In this section, we give the basic principles of our numerical method. Since each phase is treated separately, we first describe the method in the case of a one-phase problem. Then, we describe its application to the multiphase problem of Section 2.

#### 3.1. A General One-Phase Problem

We consider a general one-phase problem in a *given* variable domain.

Let  $\mathcal{R} = \{(x, t); a_L(t) < x < a_R(t), t > 0\}$ , where  $a_L(t)$  and  $a_R(t)$  are two given continuous functions of  $t$ . Let  $\mathcal{E}_L$  and  $\mathcal{E}_R$  denote the left and right boundaries of  $\mathcal{R}$ , i.e., the curves  $x = a_L(t)$  and  $x = a_R(t)$ , respectively. Let  $c$  and  $K$  be two positive



constants;  $f$  a given function defined in  $\mathcal{A}$ ;  $u_0(x)$  a given function defined for  $a_L(0) < x < a_R(0)$ ; and  $\alpha_L, \beta_L, g_L, \alpha_R, \beta_R, g_R$  six given functions of  $t$  defined for  $t > 0$  and such that  $|\alpha_s(t)| + |\beta_s(t)| > 0$  for  $t > 0$  and  $s = L$  and  $R$  (i.e.,  $\alpha_s$  and  $\beta_s$  do not vanish at the same time).

We want to solve the following problem.

$$c \frac{\partial u}{\partial t} - K \frac{\partial^2 u}{\partial x^2} = f \quad \text{in } \mathcal{A}, \tag{3.1}$$

$$u(x, 0) = u^0(x) \quad \text{for } a_L(0) < x < a_R(0), \tag{3.2}$$

$$\alpha_s u + \beta_s \frac{\partial u}{\partial x} = g_s \quad \text{on } \mathcal{C}_s, \quad \text{for } s = L \text{ and } R. \tag{3.3}$$

Let  $\{t^n; n \geq 0\}$  be a sequence such that  $t^0 = 0$  and  $t^n < t^{n+1}$  for all  $n$ . Let  $G^n, \Gamma_L^n, \Gamma_R^n, \Omega^n, \Omega^{n+1}$  be defined as indicated on Fig. 5 in the same way as the similar sets defined in Section 2.3. Let

$$B_s^n(w, \varphi) \equiv \int_{\Gamma_s^n} w \varphi dt, \quad \text{for } s = L, R, \tag{3.4}$$

and for any integrable functions  $w$  and  $\varphi$  defined on  $\Gamma_s^n$ .

Then, the integral relation (2.11) applied to the domain  $G^n$  can be written in the form

$$\mathcal{B}^n(u, \varphi) + KB_L^n \left( \frac{\partial u}{\partial x}, \varphi \right) - KB_R^n \left( \frac{\partial u}{\partial x}, \varphi \right) = \mathcal{A}^n(u, f, \varphi), \tag{3.5}$$

for all functions  $\varphi \in \Phi(G^n)$ , with

$$\begin{aligned} \mathcal{B}^n(u, \varphi) \equiv & - \iint_{G^n} cu \frac{\partial \varphi}{\partial t} dx dt + \iint_{G^n} K \frac{\partial u}{\partial x} \frac{\partial \varphi}{\partial x} dx dt \\ & + \int_{\Omega^{n+1}} cu \varphi dx + \int_{\Gamma_L^n} cu \varphi dx - \int_{\Gamma_R^n} cu \varphi dx, \end{aligned} \tag{3.6}$$

$$\mathcal{A}^n(u, f, \varphi) \equiv \int_{\Omega^n} cu \varphi dx + \iint_{G^n} f \varphi dx dt. \tag{3.7}$$

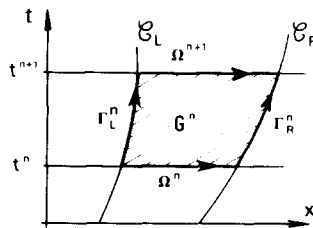


FIG. 5. The subdomain  $G^n$  and the oriented portions of its boundary.

$\mathcal{B}^n(u, \varphi)$  is a bilinear form which involves the values of  $u$  for  $t^n < t \leq t^{n+1}$ .

$B_s^n(\partial u/\partial x, \varphi)$  is a bilinear form which involves the boundary values of the derivative  $\partial u/\partial x$  for  $t^n < t < t^{n+1}$ .

$\mathcal{A}^n(u, f, \varphi)$  involves the values of  $u$  for  $t = t^n$ .

On the other hand, Eqs. (3.3) yield

$$B_s^n \left( \alpha_s u + \beta_s \frac{\partial u}{\partial x}, \varphi \right) = B_s^n(g_s, \varphi), \quad \text{for } s = L, R, \tag{3.8}$$

and for all functions  $\varphi \in \Phi(\Gamma_s^n)$ , where  $\Phi(\Gamma_s^n)$  denotes the set of all Lipschitz-continuous functions defined on  $\Gamma_s^n$ .

Our numerical method is based on the integral relations (3.5) and (3.8).

### 3.2. A General Conservative Numerical Scheme

Let  $u$  be the solution of problem (3.1), (3.2), (3.3). We want to compute an approximation of  $u$  on  $\mathcal{A}$  and an approximation of the boundary derivatives  $\partial u/\partial x|_L$  and  $\partial u/\partial x|_R$  on  $\mathcal{E}_L$  and  $\mathcal{E}_R$ , respectively. Let us denote these approximations by  $u_h$ ,  $(Du)_{h,L}$  and  $(Du)_{h,R}$ . At each time step, we know the values of  $u_h$  at the time  $t^n$  and we want to compute the values of  $u_h$ ,  $(Du)_{h,L}$  and  $(Du)_{h,R}$  for  $t^n < t \leq t^{n+1}$ .

Let  $\Phi_h(G_n)$  and  $\Phi_h(\Gamma_s^n)$  be finite dimensional subspaces of  $\Phi(G^n)$  and  $\Phi(\Gamma_s^n)$ , respectively, with  $s = L$  and  $R$ . By a method that we will specify below, we determine three functions,  $v_h \in \Phi_h(G^n)$ ,  $w_{h,L} \in \Phi_h(\Gamma_L^n)$  and  $w_{h,R} \in \Phi_h(\Gamma_R^n)$ ; then, we take

$$u_h = v_h \quad \text{and} \quad (Du)_{h,s} = w_{h,s}, \quad s = L \text{ and } R, \text{ for } t^n < t \leq t^{n+1}. \tag{3.9}$$

*Remarks.* Before specifying how we determine the functions  $v_h$  and  $w_{h,s}$ , we make two remarks:

(i) It follows from (3.9) that the function  $u_h$  is continuous in the strip  $t^n < t \leq t^{n+1}$  (since the function  $v_h$  is continuous in the strip  $t^n \leq t \leq t^{n+1}$  by definition of the space  $\Phi(G^n)$ ). But, in general, the two functions  $u_h$  and  $v_h$  do not coincide at the time  $t = t^n$  and therefore the function  $u_h$  is discontinuous at the time  $t^n$ . We will note  $u_h^{n+0} = u_h(\cdot, t^n)$  and

$$u_h^{n+0} = v_h(\cdot, t^n) = \lim\{u_h(\cdot, t^n + \varepsilon); \varepsilon > 0, \varepsilon \rightarrow 0\}.$$

(ii) Assuming that the function  $v_h$  admits a derivative  $\partial v_h/\partial x$  on the boundary  $\Gamma_s^n$ , the function  $w_{h,s}$  does not in general coincide with  $\partial v_h/\partial x$  on  $\Gamma_s^n$ . Hence,

$$(Du)_{h,s} \neq \partial u_h/\partial x|_s,$$

where  $\partial u_h/\partial x|_s$  denotes the restriction to  $\mathcal{E}_s$  of the derivative  $\partial u_h/\partial x$  for  $s = L$  and  $R$ .

*Determination of the Functions  $v_h$  and  $w_{h,s}$*

We solve the following problem.

Find  $v_h \in \Phi_h(G^n)$  and  $w_{h,s} \in \Phi_h(\Gamma_s^n)$  for  $s = L$  and  $R$  such that:

$$\mathcal{B}^n(v_h, \varphi_h) + KB_L^n(w_{h,L}, \varphi_h) - KB_R^n(w_{h,R}, \varphi_h) = \mathcal{A}^n(u_h^n, f, \varphi_h), \tag{3.10}$$

for all  $\varphi_h \in \Phi_h(G^n)$ , and

$$B_s^n(\alpha_s v_h + \beta_s w_{h,s}, \varphi_{h,s}) = B_s^n(g_s, \varphi_{h,s}), \tag{3.11}$$

for all  $\varphi_{h,s} \in \Phi_h(\Gamma_s^n)$ ,  $s = L$  and  $R$ .

Equations (3.10) and (3.11) represent a system of linear algebraic equations with a square matrix. The number of equations and the number of unknowns are equal to the sum of the dimensions of the three spaces  $\Phi_h(G^n)$ ,  $\Phi_h(\Gamma_L^n)$  and  $\Phi_h(\Gamma_R^n)$ .

*Particular Case*

Assume:

- (i) The coefficients  $\alpha_s$  and  $\beta_s$  are constant, for  $s = L$  or  $R$ .
- (ii) We choose  $\Phi_h(\Gamma_s^n)$  equal to the trace space of  $\Phi_h(G^n)$ , i.e. the space of the restrictions to  $\Gamma_s^n$  of the functions  $\varphi_h \in \Phi_h(G^n)$ .

Then:

— If  $g_s \in \Phi_h(\Gamma_s^n)$ , Eq. (3.11) is equivalent to

$$\alpha_s v_h + \beta_s w_{h,s} = g_s \quad \text{on } \Gamma_s^n. \tag{3.12}$$

— If  $g_s \notin \Phi_h(\Gamma_s^n)$ , Eq. (3.12) holds with  $g_s$  replaced by its projection  $g_{s,h}$  on the space  $\Phi_h(\Gamma_s^n)$  with respect to the inner product defined by (3.4).

These statements follow at once from the observation that, under the foregoing assumptions, we have  $\alpha_s v_h + \beta_s w_{h,s} \in \Phi_h(\Gamma_s^n)$ .

*Notation.* We will denote by  $(Du)_h$  the function defined on  $\Gamma_h^n \cup \Gamma_R^n$  such that  $(Du)_h = (Du)_{h,s}$  on  $\Gamma_s^n$ , for  $s = L$  and  $R$ .

*Conservativity of the Scheme*

Let us choose the space  $\Phi_h(G^n)$  so that it contains the functions  $\varphi_h$  which are constant. Then, taking  $\varphi_h$  identical to 1 in (3.10) and using (3.9), we get

$$-\int_{\partial G^n} (cu_h \, dx + K(Du)_h \, dt) = \iint_{G^n} f \, dx \, dt. \tag{3.13}$$

Hence, the solution of the discrete problem (3.10), (3.11) satisfies a relation of conservation analogous to (2.12) in each subdomain  $G^n$ .

*Remarks.* The way in which we approximate the derivative  $\partial u/\partial x$  on the boundaries is related to a method of Douglas *et al.* [5].

The choice of a space of test functions which contains the constants in order to get a conservative scheme was proposed by the authors [8] for solving the system of conservation laws of inviscid compressible flow. Time discontinuous Galerkin-type approximations for parabolic problems were proposed in [7].

### 3.3. Application to the Multiphase Problem

Now, we consider the multiphase problem of Section 2. We assume that the problem has been solved until the time  $t^n$  and we describe a method to solve it until the time  $t^{n+1}$ . We assume that the two moving boundaries  $\mathcal{C}_1$  and  $\mathcal{C}_2$  exist at the times  $t^n$  and  $t^{n+1}$ . The treatment of appearing and disappearing phases will be described in detail in the next section.

#### Step 1

First, we assume that the moving boundaries are known. In each phase, we have to solve a problem of the form (3.1), (3.2), (3.3) with the boundary conditions given by (2.3), (2.6) and (2.7).

For each phase, let us define the sets  $G_j^n$ ,  $\Gamma_{j-1}^n = \Gamma_{j,L}^n$ ,  $\Gamma_j^n = \Gamma_{j,R}^n$ ,  $\Omega_j^n$  and  $\Omega_j^{n+1}$ , for  $j = 1$  and  $2$ , as in Section 3.2. (The notations are the same as in Section 2.3, except for the index  $n$  which has been added since  $(\tau, \tau') = (t^n, t^{n+1})$ . See Figs. 4 and 5.) Let  $\Phi_h(G_j^n)$  and  $\Phi_h(\Gamma_j^n)$  be finite dimensional subspaces of  $\Phi(G_j^n)$  and  $\Phi(\Gamma_j^n)$  for  $j = 1, 2$  and  $j' = 0, 1, 2$ , which satisfy the following hypotheses.

(H1) Each space  $\Phi_h(\Gamma_{j'}^n)$  is equal to the trace space of the corresponding space  $\Phi_h(G_j^n)$  on  $\Gamma_{j'}^n$  (in particular, the trace spaces of  $\Phi_h(G_1^n)$  and  $\Phi_h(G_2^n)$  on  $\Gamma_1^n$  are both equal to  $\Phi_h(\Gamma_1^n)$ ).

(H2) The spaces  $\Phi_h(G_j^n)$  contain the functions which are identical to constants.

*Notation.* For each domain  $G_j^n$ , we denote

$$\begin{aligned} \bar{G}_j^n &= \text{closure of } G_j^n, \\ \tilde{G}_j^n &= \bar{G}_j^n - \Omega^n = \{(x, t); (x, t) \in \bar{G}_j^n, t^n < t \leq t^{n+1}\}. \end{aligned}$$

We will also denote by  $\bar{\Gamma}_j^n$  the closure of  $\Gamma_j^n$ .

The application of the method of Section 3.2 to each of the phases gives

$$\begin{aligned} (u_h)_j &= \text{approximation of } u \text{ on } \tilde{G}_j^n, \\ (Du)_{j,h} &= \text{approximation of } \left( \frac{\partial u}{\partial x} \right)_j \text{ on } \Gamma_{j-1}^n \cup \Gamma_j^n. \end{aligned}$$

According to the particular case of Section 3.2, hypotheses H1 and H2 imply that  $(u_h)_1 = (u_h)_2 = u_m$  on  $\Gamma_1^n$ . Hence, taking  $u_h = (u_h)_j$  on  $\tilde{G}_j^n$ , we get a function  $u_h$  which is defined and continuous on  $\tilde{G}_1^n \cup \tilde{G}_2^n$ .

*Step 2. Approximation of the moving boundaries*

The moving boundaries  $\mathcal{E}_1$  and  $\mathcal{E}_2$  are determined by the differential equations (2.8) and (2.9) which are of the form

$$\frac{da}{dt} = \mathcal{F} \left( \left( \frac{\partial u}{\partial x} \right)_1, \left( \frac{\partial u}{\partial x} \right)_2, t \right), \tag{3.14}$$

with  $a = a_j$ ,  $j = 1$  or  $2$  and  $\mathcal{F} = \mathcal{F}_j$  a functional which involves the values of  $(\partial u / \partial x)_1$  and  $(\partial u / \partial x)_2$  on  $\mathcal{E}_j$ .

For each  $n \geq 0$ , let  $\mathcal{S}_h(t^n, t^{n+1})$  be a finite dimensional space of continuous functions defined on the interval  $[t^n, t^{n+1}]$ . We want to approximate each function  $a(t)$  by a continuous function  $a_h(t)$  which coincides with a function of  $\mathcal{S}_h(t^n, t^{n+1})$  on each interval  $[t^n, t^{n+1}]$ . At each time step, the initial value  $a_h(t^n)$  is known and we must determine the values of  $a_h$  for  $t^n < t \leq t^{n+1}$ .

Let us replace Eq. (3.14) by

$$d\tilde{a}/dt = \mathcal{F}((Du)_{1,h}, (Du)_{2,h}, t), \tag{3.15}$$

obtained by replacing  $(\partial u / \partial x)_1$  and  $(\partial u / \partial x)_2$  by their approximations in the right-hand-side member of (3.14). Then,  $a_h$  is determined by computing an approximate solution of (3.15) which belongs to the space  $\mathcal{S}_h(t^n, t^{n+1})$ . The numerical method used for computing  $a_h$  in relation with a particular choice of the space  $\mathcal{S}_h(t^n, t^{n+1})$  will be specified in the next section.

At each time step, the numerical solution of the complete multiphase problem involves iterations based on Steps 1 and 2. The iterations are started by making an initial guess for the moving boundaries.

*Conservativity*

Assume that, for each boundary  $\mathcal{E}_1$  and  $\mathcal{E}_2$ , the approximate solution  $a_h$  of Eq. (3.15) satisfies

$$a_h(t^{n+1}) - a_h(t^n) = \int_{t^n}^{t^{n+1}} \mathcal{F}((Du)_{1,h}, (Du)_{2,h}, t) dt. \tag{3.16}$$

*Then, the approximate solution  $u_h$  satisfies the conservation relation (2.17) exactly.*

*Proof.* In each phase the discrete relation of conservation (3.13) is satisfied; it can be written in a form analogous to (2.13). Moreover, the condition (3.16) is the discrete analogue of (2.14) and (2.15). Finally, hypotheses H1 and H2 imply that the boundary conditions (2.3), (2.6) and (2.7) are satisfied exactly, according to the particular case of Section 3.2, i.e.,  $(Du)_{1,h} = 0$  on  $\Gamma_0^n$ ,  $u_h = u_m$  on  $\Gamma_1^n$  and  $u_h = u_v$  on  $\Gamma_2^n$ . The conservation relation (2.17) follows for the function  $u_h$  as is Section 2.3.

### *Use of Numerical Quadrature Formulae*

Instead of computing the exact value of the integrals which are involved in the definition of the functionals  $\mathcal{A}^n$ ,  $\mathcal{B}^n$  and  $B_s^n$  (formulae (3.7), (3.6) and (3.4)), we will use numerical quadrature formulae. Then, if the assumptions H1, H2 and (3.16) are satisfied, the approximate solution  $u_h$  satisfies an approximate form of the conservation relation (2.17) in which the integrals have been replaced by their approximate value. But, we will choose the quadrature formulae in such a way that the integrals involved in this relation are computed exactly. In this case, despite the use of quadrature formulae, the approximate solution  $u_h$  satisfies the conservation relation (2.17) *exactly*.

A choice of numerical quadrature formulae which satisfy this property in relation with the choice of the discrete function spaces will be specified in the next section.

## 4. FINITE ELEMENTS

In the previous section, we have described the principle of a numerical method to solve the problem of Section 2. In order to determine this method completely, it remains to specify the following points:

- choice of the discrete function spaces,
- choice of the numerical quadrature formulae,
- choice of a numerical method to solve the differential equation (3.15),
- algorithm for solving the system of discrete equations,
- special arrangements concerning the computation of appearing and disappearing phases.

This section is based on finite elements in space and time.

### 4.1. *Choice of the Discrete Spaces*

First, we take the space  $\mathcal{S}_h(t^n, t^{n+1})$  equal to the space of all functions defined in the interval  $[t^n, t^{n+1}]$  which coincide with a polynomial of degree  $\leq 2$ . Hence, each moving boundary is approximated in the interval  $[t^n, t^{n+1}]$  by an arc of parabola  $\Gamma_j^n$  of the form  $x = a_h(t)$ , where  $a_h(t)$  is a polynomial of degree  $\leq 2$ .

The definition of the spaces  $\Phi_h(G_j^n)$  and  $\Phi_h(\Gamma_j^n)$  is based on a partition of each of the domains  $G_1^n$  and  $G_2^n$  into isoparametric quadrilateral finite elements of type (2) (see [4, p. 231]), according to the method of [1] that we will recall.

Let  $\mathcal{E}_h^n$  denote the set of the finite elements which correspond to the time step  $n$ . Each element  $K = K_i^n \in \mathcal{E}_h^n$  admits two vertices  $P_i^{n+0}$  and  $P_{i+1}^{n+0}$  on the line  $t = t^n$  and two vertices  $P_i^{n+1}$  and  $P_{i+1}^{n+1}$  on the line  $t = t^{n+1}$ , where  $i$  is a space index. The vertices  $P_i^{n+0}$  of the elements  $K_i^n \in \mathcal{E}_h^n$  should not be confused with the vertices  $P_i^n$  of the elements  $K_i^{n-1} \in \mathcal{E}_h^{n-1}$  corresponding to the previous step; at each time step, the

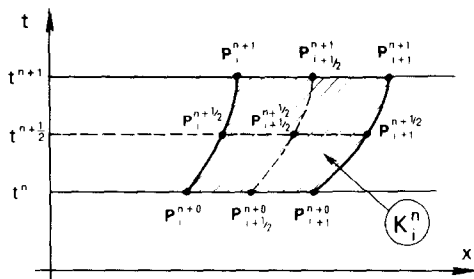


FIG. 6. A finite element  $K_i^n$ .

choice of the finite elements is *arbitrary* and can be made without any connection with the choice of the finite elements at the previous step; hence, the vertices  $P_i^n$  and  $P_i^{n+0}$  may be distinct. Each element  $K_i^n$  admits two straight sides  $\overline{P_i^{n+0}P_{i+1}^{n+0}}$  and  $\overline{P_{i+1}^{n+1}P_{i+1}^{n+1}}$  and two curved sides  $\overline{P_i^{n+0}P_{i+1}^{n+1}}$  and  $\overline{P_{i+1}^{n+0}P_{i+1}^{n+1}}$ . Each curved side  $\overline{P_i^{n+0}P_{i+1}^{n+1}}$  is common to two adjacent elements  $K_{i-1}^n$  and  $K_i^n$ ; it is an arc of parabola of the form  $x = x_i(t)$ , where  $x_i(t)$  is a polynomial of degree  $\leq 2$ . (See Fig. 6).

Each point  $P = (x, t) \in K_i^n$  can be characterized by means of two parameters  $\xi$  and  $\eta$  defined by

$$\xi = \frac{x - x_i(t)}{x_{i+1}(t) - x_i(t)}, \quad \eta = \frac{t - t^n}{t^{n+1} - t^n}. \tag{4.1}$$

This formula defines a one-to-one correspondence between the points  $P = (x, t)$  of the element  $K_i^n$  and the points  $\hat{P} = (\xi, \eta)$  of the square  $\hat{K} = \{(\xi, \eta); 0 \leq \xi \leq 1, 0 \leq \eta \leq 1\}$ . Let us denote by  $P_{i+\mu}^{n+\nu}$  the nine points of the element  $K_i^n$  which correspond to  $\xi = \mu$  and  $\eta = \nu$ , with  $\mu$  and  $\nu$  equal to 0,  $\frac{1}{2}$  or 1. These points are called the nodes of the element  $K_i^n$ .

Let  $Q_2(K)$  be the space of all functions defined on the element  $K = K_i^n$  which can be written in the form of a polynomial  $q_2(\xi, \eta)$  of degree  $\leq 2$  with respect to each of the variables  $\xi$  and  $\eta$  separately. We choose the spaces  $\Phi_h$  in the following way.

$\Phi_h(G_j^n)$  = the space of all functions defined and continuous on  $\bar{G}_j^n$ , for  $j = 1$  and  $2$ , and such that their restriction to each element  $K$  belongs to  $Q_2(K)$ .

$\Phi_h(\Gamma_j^n)$  = the space of the traces on  $\Gamma_j^n$  of the functions of

$\Phi_h(G_1^n)$  or  $\Phi_h(G_2^n)$ , for  $j = 0, 1, 2$ ,

= the space of all functions defined on  $\Gamma_j^n$  which coincide with a polynomial  $p_2(t)$  of degree  $\leq 2$ .

The functions of  $\Phi_h(G_j^n)$  and  $\Phi_h(\Gamma_j^n)$  are uniquely determined by their values on the set of the nodes  $P_{i+\mu}^{n+\nu}$  which belong to  $\bar{G}_j^n$  and  $\bar{\Gamma}_j^n$ , respectively.

Note that the spaces  $\Phi_h(G_j^n)$  and  $\Phi_h(\Gamma_j^n)$  contain the constant functions. The hypotheses H1 and H2 of Section 3.3 are satisfied.

## 4.2. Numerical Quadrature Formulae

For each element  $K$ , we use the following quadrature formulae in which  $\psi$  is an arbitrary function defined on  $K$  and  $\psi_{i+\mu}^{n+\nu} = \psi(P_{i+\mu}^{n+\nu})$ .

(a) Integrals with respect to  $x$  for fixed  $t$ :

$$\int_{P_i^{n+\nu}}^{P_{i+1}^{n+\nu}} \psi(x, t^{n+\nu}) dx \sim J_i^{n+\nu}(\psi), \quad (4.2)$$

with

$$J_i^{n+\nu}(\psi) = \frac{1}{6}(x_{i+1}^{n+\nu} - x_i^{n+\nu})(\psi_i^{n+\nu} + 4\psi_{i+1/2}^{n+\nu} + \psi_{i+1}^{n+\nu})$$

(Simpson's rule).

(b) Integrals along the curved sides of the elements  $K$ :

$$\int_{P_i^{n+0}}^{P_i^{n+1}} \psi(x_i(t), t) dt \sim \frac{1}{6}(t^{n+1} - t^n)(\psi_i^{n+0} + 4\psi_i^{n+1/2} + \psi_i^{n+1}). \quad (4.3)$$

(c) Integrals in  $K$ :

$$\iint_{K_i^n} \psi(x, t) dx dt \sim \frac{1}{6}(t^{n+1} - t^n)(J_i^{n+0}(\psi) + 4J_i^{n+1/2}(\psi) + J_i^{n+1}(\psi)). \quad (4.4)$$

Note that the quadrature formulae (4.2) and (4.3) are exact for all functions  $\psi$  which belong to  $Q_2(K)$ .

## 4.3. COMPUTATION OF THE MOVING BOUNDARIES

Following the general method described in Section 3.3, we want to approximate the solution  $\tilde{a}(t)$  of the differential equation (3.15) in the interval  $[t^n, t^{n+1}]$  by a function  $a_h \in \mathcal{S}_h(t^n, t^{n+1})$ , i.e., a polynomial of degree  $\leq 2$ . Such a polynomial is uniquely determined by its values for  $t = t^{n+\nu}$ ,  $\nu = 0, \frac{1}{2}, 1$ . The initial value of  $a_h(t)$  for  $t = t^n$  is known. Therefore, it is sufficient to compute  $a_h(t^{n+\nu})$  for  $\nu = \frac{1}{2}$  and 1.

The differential equation (3.15) with the initial condition  $\tilde{a}(t^n) = a_h(t^n)$  yields

$$\tilde{a}(t^{n+\nu}) = a_h(t^n) + \int_{t^n}^{t^{n+\nu}} \mathcal{F}((Du)_{1,h}, (Du)_{2,h}, t) dt, \quad (4.5)$$

where the integrated function is equal to

$$\mathcal{F}_1((Du)_{1,h}, (Du)_{2,h}, t) \equiv (K_1(Du)_{1,h} - K_2(Du)_{2,h})/C_m,$$



on the moving boundary  $\mathcal{E}_1$ , and

$$\mathcal{F}_2((Du)_{1,h}, (Du)_{2,h}, t) \equiv (K_2(Du)_{2,h} - F(t))/C_v,$$

on the moving boundary  $\mathcal{E}_2$ .

The functions  $(Du)_{1,h}$  and  $(Du)_{2,h}$  are equal to polynomials of degree  $\leq 2$  in the interval  $[t^n, t^{n+1}]$ ; therefore, it is easy to integrate them exactly. Let us assume that the function  $F(t)$  can also be integrated exactly. Then, we compute the right-hand-side member of (4.5) exactly and we take

$$a_h(t^{n+\nu}) = \tilde{a}(t^{n+\nu}) \quad \text{for } \nu = \frac{1}{2} \text{ and } 1. \tag{4.6}$$

Relation (3.16) is satisfied; therefore the approximate solution  $u_h$  satisfies the conservation relation (2.17) exactly in the interval  $[t^n, t^{n+1}]$ .

If the function  $F(t)$  cannot be integrated exactly, the conservation relation (2.17) is satisfied with the right-hand-side member  $E_6$  replaced by its approximated value.

#### 4.4. Algorithm for Solving the Discrete Problem

At each time step, we use an iterative procedure to solve the system of algebraic equations corresponding to the discrete problem. Each iteration consists of two steps as indicated in Section 3.3. We will consider each of these steps separately and indicate the initial guess used for starting the iterations.

##### Step 1: Computation of the Functions $u_h$ and $(Du)_h$

Assume that the moving boundaries are given for  $t^n \leq t \leq t^{n+1}$ . For each of the domains  $G_1^n$  and  $G_2^n$  we must solve the functions  $u_h$  and  $(Du)_h$  which satisfy Eqs. (3.10) and (3.11). Since these functions are uniquely determined by their values at the nodes, we can write Eqs. (3.10) and (3.11) in terms of the nodal values.

Let  $\Sigma^n$  denote the set of the nodes of all elements  $K \in \mathcal{E}_h^n$  and let  $I_j = I_j(n)$  be the number of elements  $K \in \mathcal{E}_h^n$  which are contained in  $\bar{G}_j^n$ , for  $j = 1$  or  $2$ . For each domain  $G_j^n$ , we have  $\Gamma_L^n = \Gamma_{j-1}^n$ ,  $\Gamma_R^n = \Gamma_j^n$  and the unknowns are

- the values of  $v_h$  at the nodes  $P \in \Sigma^n \cap \bar{G}_j^n$ , i.e.,  $3(2I_j + 1)$  unknowns,
- the values of  $w_{h,L}$  at the nodes  $P \in \Sigma^n \cap \bar{\Gamma}_{j-1}^n$ , i.e., 3 unknowns,
- the values of  $w_{h,R}$  at the nodes  $P \in \Sigma^n \cap \bar{\Gamma}_j^n$ , i.e., 3 unknowns.

Writing Eqs. (3.10) and (3.11) for each of the functions  $\phi_h$ ,  $\phi_{h,L}$  and  $\phi_{h,R}$  which are equal to 1 at one node and vanish at the others, we get a system of linear algebraic equations with a square matrix of order  $6I_j + 9$ . This system is solved by means of Gauss method arranged in a way which takes advantage of the band structure of the matrix (see Appendix 1 of [1] for the explicit expression of Eq. (3.10) in the case of interior nodes).

Let us recall that, according to the particular case of Section 3.2, Eqs. (3.11) are equivalent to  $w_{h,L} = 0$  on  $\Gamma_0^n$ ,  $v_h = u_m$  on  $\Gamma_1^n$  and  $v_h = u_v$  on  $\Gamma_2^n$ .

For each domain  $G_j^n$ , we take  $u_h = v_h$  on  $\tilde{G}_j^n$ ,  $(Du)_{j,h} = w_{h,L}$  on  $\Gamma_{j-1}^n$  and  $(Du)_{j,h} = w_{h,R}$  on  $\Gamma_j^n$ .

*Step 2: Computation of the Moving Boundaries*

For each moving boundary, we must compute the values of  $a_h(t^{n+v})$  for  $v = \frac{1}{2}$  and 1. Let  $a_h^{(l)}(t^{n+v})$  be the values which have been computed at the iteration  $l$ , where  $l$  is the iteration number. Let  $u_h^{(l)}$  and  $(Du)_{j,h}^{(l)}$  be the corresponding values of  $u_h$  and  $(Du)_{j,h}$  which have been computed in Step 1. We compute  $a_h^{(l+1)}(t^{n+v})$  by means of an auxiliary value  $\hat{a}_h^{(l+1)}(t^{n+v})$  in the following way.

$$\hat{a}_h^{(l+1)}(t^{n+v}) = a_h(t^n) + \int_{t^n}^{t^{n+v}} \mathcal{F}((Du)_{1,h}^{(l)}, (Du)_{2,h}^{(l)}, t) dt, \tag{4.7}$$

$$a_h^{(l+1)}(t^{n+v}) = (1 - \omega) a_h^{(l)}(t^{n+v}) + \omega \hat{a}_h^{(l+1)}(t^{n+v}), \tag{4.8}$$

where  $\omega$  is a parameter,  $0 < \omega \leq 1$ .

It seems natural to take  $\omega = 1$ ; but, in some cases, it is necessary to take  $\omega < 1$  in order to get convergent iterations. The choice  $\omega = 0.5$  has been satisfactory for all the computations that we have made.

*Iteration Start*

For starting the iterations, we choose the function  $a_h$  as follows.

— If  $n \geq 1$ , we extrapolate the values of  $a_h$  corresponding to the previous time step: i.e., we take  $a_h$  equal to the same polynomial as in the interval  $[t^{n-1}, t^n]$ .

— If  $n = 0$ , we take  $a_h^{(0)}(t) = a_h(0) + S^0 t$ , with  $S^0 = \mathcal{F}((\partial u^0/\partial x)_1, (\partial u^0/\partial x)_2, 0)$  = initial speed of propagation of the moving boundary.

**4.5. Appearance of a Phase**

A phase appears when the temperature on the fixed boundary  $x = a$  becomes superior either to the melting temperature  $u_m$  or to the vaporization temperature  $u_v$ .

*4.5a. Computation of the Time of Appearance of a Phase*

Let us consider the values  $u_h(a, t^n)$  computed on the fixed boundary  $x = a$  for increasing values of  $n$ . Let  $\Delta t^n = t^{n+1} - t^n$ . If, for a certain value of  $n$  and for a certain value  $\Delta t$  of the time step  $\Delta t^n$ , we get

$$u_h(a, t^n) < u_m \leq u_h(a, t^n + \Delta t),$$

the appearance of the liquid phase occurs in the time interval  $(t^n, t^n + \Delta t]$ . Then, we change the value of the time step  $\Delta t^n$  in such a way that

$$u_h(a, t^{n+1}) = u_m. \tag{4.9}$$

The new value of  $t^{n+1}$  approximates the time  $t_m$  at which the new phase appears.

In (4.9), we take  $u_h$  equal to the function which has been computed with the first value  $\Delta t$  of the time step  $\Delta t^n$ . This equation is a polynomial equation of degree  $\leq 2$  and it admits a unique solution  $t^{n+1} \in (t^n, t^n + \Delta t]$ . For simplicity, we do *not* iterate Eq. (4.9) by replacing  $u_h$  by the new computed function corresponding to the new value of the time step  $\Delta t^n$ . The numerical experiments have shown that such iterations are unnecessary.

We proceed in the same way for computing the time of appearance of the vapor phase (replace  $u_m$  by  $u_v$ ).

4.5b. *Computation of the Appearing Phase*

The computation of the temperature in the appearing phase must be done only for the liquid phase, since the vapor phase is eliminated as soon as it appears.

Let  $t^n$  be the computed value of the time at which the liquid phase appears. At the next time step, we want to compute the position  $a_h(t) = a_{1,h}(t)$  of the moving boundary in the interval  $(t^n, t^{n+1}]$  and the temperature  $u_h$  in each of the phases. We use the general method of Section 3.3 in the following way.

*Choice of the space  $\Phi_h(G_2^n)$ .* The domain  $G_2^n$  which corresponds to the liquid phase is approximated by a single curved triangular element  $K$ . The vertices of  $K$  are the points  $P_i^n = P_{i+1}^n = (a, t^n)$ ,  $P_{i+1}^{n+1} = (a_h(t^{n+1}), t^{n+1})$  and  $P_{i+1}^{n+1} = (a, t^{n+1})$ . The sides  $\frac{P_i^n P_{i+1}^{n+1}}$  and  $\frac{P_{i+1}^{n+1} P_{i+1}^{n+1}}$  are straight and coincide with the lines  $x = a$  and  $t = t^{n+1}$

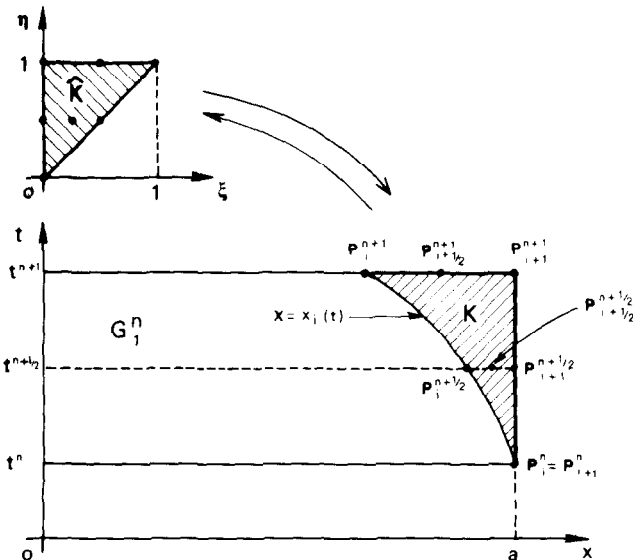


FIG. 7. Appearance of the liquid phase: the curved triangular element  $K = \bar{G}_2^n$  and the corresponding triangle  $\bar{K}$ .

respectively; the side  $\widehat{P_i^n P_{i+1}^{n+1}}$  is an arc of parabola  $x = x_i(t) = a_h(t)$  which coincides with the moving boundary (see Fig. 7).

Each point  $P = (x, t) \in K$  can be characterized by means of two parameters  $\xi$  and  $\eta$  defined by the formulae

$$\eta = \frac{t - t^n}{t^{n+1} - t^n}, \quad \xi = \eta \frac{x - x_i(t)}{a - x_i(t)}. \tag{4.10}$$

These formulae establish a one-to-one correspondence between the points  $P = (x, t) \in K$  and the points  $\hat{P} = (\xi, \eta)$  of the triangle  $\hat{K} = \{(\xi, \eta); 0 \leq \xi \leq \eta \leq 1\}$ . Let us remark that the coordinates  $x$  and  $t$  can be written in the form of polynomials of degree  $\leq 2$  in  $\xi$  and  $\eta$  (since  $a - x_i(t)$  is a polynomial of degree  $\leq 2$  in  $t$  which vanishes for  $t = t^n$ ).

Let  $P_i^{n+1/2} = (a_h(t^{n+1/2}), t^{n+1/2})$ ,  $P_{i+1}^{n+1/2} = (a, t^{n+1/2})$  and  $P_{i+\nu}^{n+\nu} = \frac{1}{2}(P_i^{n+\nu} + P_{i+1}^{n+\nu})$  for  $\nu = \frac{1}{2}$  and 1, with  $t^{n+1/2} = \frac{1}{2}(t^n + t^{n+1})$ . The seven points  $P_i^n$  and  $P_{i+\mu}^{n+\nu}$  for  $\mu \in \{0, \frac{1}{2}, 1\}$  and  $\nu \in \{\frac{1}{2}, 1\}$  are called the nodes of the finite element  $K$ .

We choose the space  $\Phi_h(G_2^n)$  equal to the set of all functions  $\phi_h$  which are defined on  $K = \bar{G}_2^n$  and which can be written in terms of the variables  $\xi$  and  $\eta$  as a linear combination of the seven functions  $\{1, \xi, \eta, \xi^2, \xi\eta, \eta^2, \xi(\xi - \eta)\eta\}$ . It is easy to check that an arbitrary function of  $\Phi_h(G_2^n)$  is uniquely determined by its values at the seven nodes of the element  $K$ . The element  $K$  is an example of a subparametric finite element.

The spaces  $\Phi_h(\Gamma_i^n)$  are chosen as in Section 4.1.

*Quadrature formulae.* For computing the integrals in the triangular element  $K$ , we use the quadrature formula (4.4) with  $J_i^{n+0}(\psi) = 0$ .

Let us remark that the corresponding quadrature formula in the triangle  $\hat{K}$  is exact for all polynomials of degree  $\leq 2$  in  $\xi$  and  $\eta$ . This property may seem surprising at first sight since the value of the integrated function at the origin does not appear in the formula. The reason is that the polynomial  $\hat{\psi}(\xi, \eta) = (1 - 2\eta)(1 - \eta)$  which is equal to 1 at the origin and vanishes at the other nodes of  $\hat{K}$  admits a vanishing integral on  $\hat{K}$ .

*Numerical solution of the discrete problem.* Writing Eqs. (3.10) and (3.11) for the triangular domain  $G_2^n$ , we get a system of 13 linear algebraic equations whose unknowns are:

- the values of  $v_h$  at the seven nodes of the element  $K = \bar{G}_2^n$ ,
- the values of  $w_{h,L}$  at the three nodes located on  $\bar{\Gamma}_L^n = \bar{\Gamma}_1^n$  (moving boundary),
- the values of  $w_{h,R}$  at the three nodes located on  $\bar{\Gamma}_R^n$  (fixed boundary).

According to the particular case of Section 3.2, Eqs. (3.11) yield

$$v_h = u_m \text{ on } \Gamma_L^n, \quad w_{h,R} = F_h(t)/K_2 \text{ on } \Gamma_R^n,$$

where  $F_h$  is the projection of the function  $F$  on the space  $\Phi_h(\Gamma_R^n)$ .

The remaining unknowns are the values of  $v_h$  at the four nodes which are not located on the moving boundary  $\bar{\Gamma}_1^n$  and the values of  $w_{h,L}$  at the three nodes which are located on  $\bar{\Gamma}_1^n$ . The corresponding system of equations is solved by Gauss method and we take:

$$u_h = v_h \text{ on } \tilde{G}_2^n \quad \text{and} \quad (Du)_{2,h} = w_{h,s} \text{ on } \Gamma_s^n \text{ with } s = L \text{ and } R.$$

Let us remark that the function  $(Du)_{2,h}$  which approximates the derivative  $(\partial u / \partial x)_2$  on  $\Gamma_L^n \cup \Gamma_R^n$  admits two distinct limit values at the point  $P_i^n$  since  $w_{h,L}(P_i^n) \neq w_{h,R}(P_i^n)$  in general.

*Computation of the moving boundary.* The moving boundary  $\Gamma_1^n$  is computed according to the method of Section 4.3, by means of the iterative algorithm of Section 4.4. For starting the iterations, we take

$$a_h^{(0)}(t) = a - \sigma(t - t^n), \tag{4.11}$$

with  $\sigma = \theta F(t^n) / C_m$ , where  $\theta$  is a parameter,  $0 < \theta < 1$ .

The choice of  $\sigma$  is derived from formula (2.8). We have replaced the term  $K_2(\partial u / \partial u)_2$  by its value on the fixed boundary given by (2.5) and the term  $K_1(\partial u / \partial x)_1 > 0$  by zero. Thus, we get an upper bound for the speed of propagation of the moving boundary. But, if the coefficient  $\sigma$  of (4.11) is chosen too large, it happens that the following iteration sends the iterated moving boundary on the other side of the fixed boundary  $x = a$  and the computations cannot proceed. Therefore, it has been useful to introduce the parameter  $\theta$ . The choice  $\theta = 1/10$  has been satisfactory for all our experiments.

Formula (4.11) is also used for starting the iterations of the appearing moving boundary  $\mathcal{E}_2$  at the time  $t_v$  at which vaporization occurs; then,  $C_m$  must be replaced by  $C_v$  in the expression of  $\sigma$ .

#### 4.6. Expansion, Reduction and Disappearance of the Phases

##### 4.6a. Choice of the Finite Elements According to the Size of the Phases

In order to follow the evolution of each phase, it is necessary to take a variable number of finite elements. We proceed in the following way.

For each of the domains  $G_1^n$  and  $G_2^n$ , we use nodes  $P_i^{n+v}$  which are equally spaced along each line  $t = t^{n+v}$ . Let  $h_j^{n+v}$  denote the distance between two consecutive nodes  $P_i^{n+v}$  and  $P_{i+1}^{n+v}$  in  $\bar{G}_j^n$ , for  $j = 1$  and  $2$ . Let  $h$  be a given positive number. The number  $I_j(n)$  of elements  $K \in \bar{G}_j^n$  is chosen equal to an integer power of 2, i.e., a number of the form  $2^p$ ,  $p$  integer. This number is determined by the condition

$$\begin{aligned} \text{either} \quad & h/2 < h_j^{n+0} \leq h, \\ \text{or} \quad & h_j^{n+0} = \text{diam } \Omega_j^n \leq h/2, \end{aligned} \tag{4.12}$$

where  $\text{diam } \Omega_j^n$  denotes the length of the interval  $\Omega_j^n$  (in the second case of (4.12), we have  $I_j(n) = 1$ ).

~~Thus, the number  $I(n)$  can be multiplied or divided by 2 at each time step if the domain  $G_j^n$  is expanding or shrinking (respectively).~~

On the other hand, we choose the time step  $\Delta t^n = t^{n+1} - t^n$  sufficiently small so that the displacement  $\Delta a_j^n$  of each moving boundary between the times  $t^n$  and  $t^{n+1}$  satisfies

$$|\Delta a_j^n| < h. \quad (4.13)$$

This condition prevents the finite elements from being too distorted. It is not a sharp condition and it need not be satisfied exactly at each time step. It could be replaced by other conditions which would limitate the distortion of the elements. This limitation is necessary for the accuracy of the method, but not for its stability. A mathematical proof of unconditional stability for a simplified problem is given in [7] and corresponding experiments are reported in [1].

#### 4.6b. Disappearance of a Phase

In our problem, only the solid phase disappears. This phenomenon occurs when the free boundary  $\mathcal{E}_1$  meets the fixed boundary  $\mathcal{E}_0$ . The corresponding time  $t_f$  is computed in the following way.

At each time step, we extend to the time interval  $[t^n, t^{n+1}]$  the arc of parabola  $I_1^{n-1}$  which approximates the moving boundary  $\mathcal{E}_1$  in the interval  $[t^{n-1}, t^n]$ . If this arc of parabola intersects the fixed boundary  $\mathcal{E}_0$ , the disappearance of the solid phase occurs in the interval  $(t^n, t^{n+1}]$ . Then, we change the time step  $\Delta t^n$  so that the new value of  $t^{n+1}$  corresponds to the intersection point (in case there would exist two intersection points, we would take the first one, i.e., the one which corresponds to the smallest value of  $t$ ). This computed value of  $t^{n+1}$  approximates the final time  $t_f$ . The values of the temperature  $u_h$  at the time  $t_f$  are computed by the method of Section 4.4 applied to the domain  $G_2^n$  which corresponds to the liquid phase. No computation is made in the domain  $G_1^n$  which corresponds to the disappearing solid phase.

*Remark.* The procedure for computing each of the times  $t_m$ ,  $t_v$ , and  $t_f$  is based on quadratic extrapolation using values computed at the previous time step, which yields an error of order 3. If a similar error was made at each time step, the method would be only of order 2. But, since this error occurs only a finite number of times (three times at most), the overall accuracy of the method remains of order 3.

## 5. NUMERICAL EXPERIMENTS

In this section, we describe the numerical experiments which have been performed for two cases of the problem of Section 2. In the first case, which corresponds to a material which is a poor heat conductor, vaporization occurs before the disappearance of the solid phase. In the second case, which corresponds to a good heat

conductor, the solid phase disappears before the appearance of vapor. For simplicity, since we are more interested in the numerical method itself than in the physical significance of the results, we will not specify the physical units which are used.

5.1. Problem 1

We consider the multiphase problem of Section 2 with the following choice of the data:

$$a_1 = 1, \quad u^0(x) = u^0 = 27, \quad F(t) = F = 2500.$$

The material is characterized by the constants:

$$\begin{aligned} c_1 = c_2 = 4944, \quad K_1 = K_2 = 0.259, \quad C_m = 2160, \\ C_v = 37200, \quad u_m = 1454, \quad u_v = 3000. \end{aligned}$$

First, we give numerical results which have been obtained for  $\Delta t = h = 1/16$ . We have taken all the time steps equal to  $\Delta t$  except at the times of appearance and disappearance of a phase. Let  $t_j \in (n\Delta t, (n+1)\Delta t)$  be the time of appearance of a phase computed as indicated in Section 4.5; then, we take two time steps corresponding to the intervals  $(n\Delta t, t_j)$  and  $(t_j, (n+1)\Delta t)$ . In this way, the values of  $t^n$  remain integer multiples of  $\Delta t$  after the appearance of the new phase.

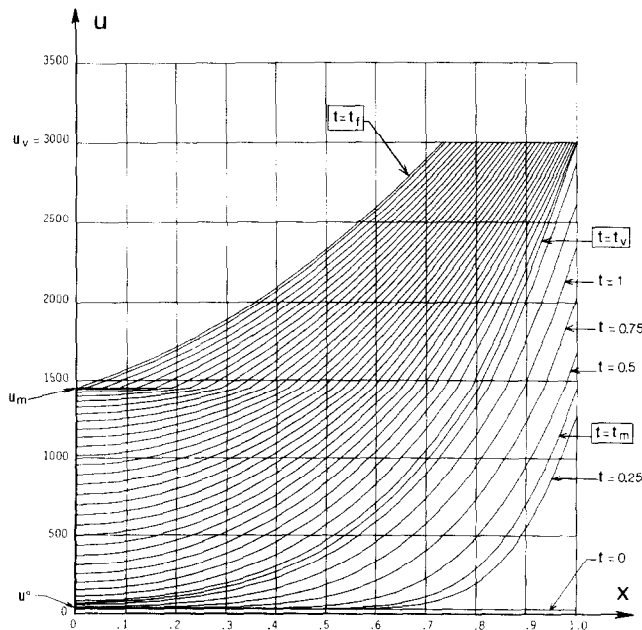


FIG. 8. Problem 1. The temperature  $u(x, t)$  for fixed values of  $t$  (computed with  $\Delta t = h = 1/16$ ).

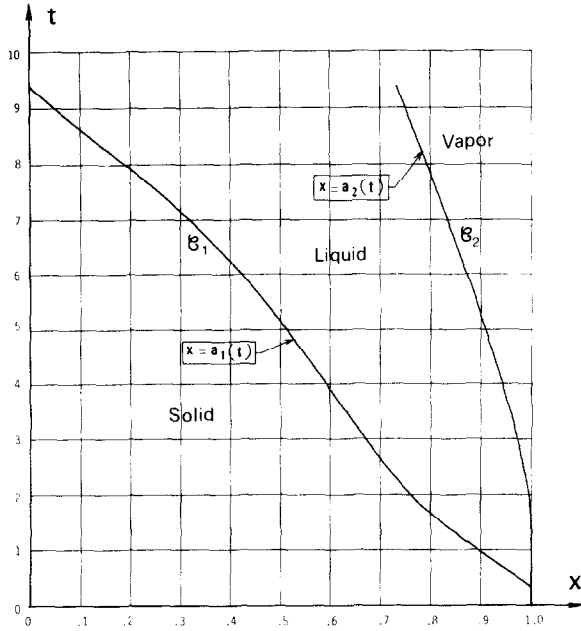


FIG. 9. Problem 1. Appearance, movement and disappearance of the free boundaries ( $\Delta t = h = 1/16$ ).

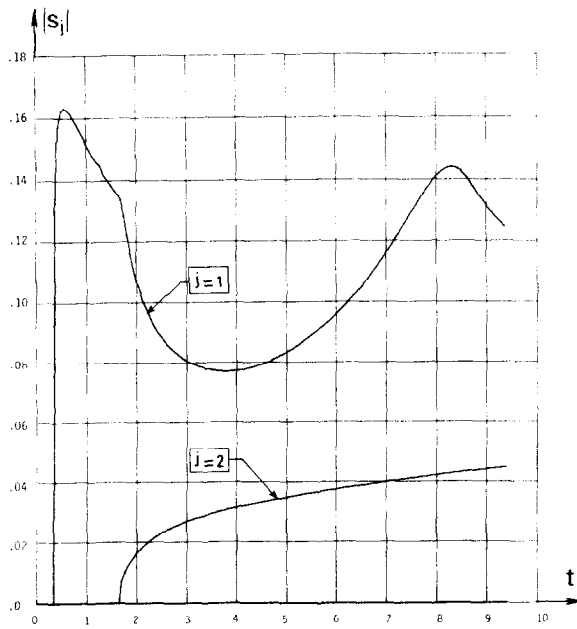


FIG. 10. Problem 1. Speed of the free boundaries:  $S_j = da_j/dt$  (computed with  $\Delta t = h = 1/16$ ).



The curves of Fig. 8 represent the computed temperature  $u_h(x, t)$  for fixed values of  $t$  equal to  $t_m, t_v, t_f$  and to integer values of  $4\Delta t$ . Figure 9 represents the displacement of the moving boundaries and Fig. 10 represents the speed of the moving boundaries, i.e., the function

$$S_{j,h}(t) \equiv \mathcal{F}_j((Du)_{1,h}, (Du)_{2,h}, t), \quad \text{for } j = 1 \text{ and } 2.$$

In the numerical solution of the discrete problem, we have used the following test for stopping the iterations:

$$|(S_{j,h}^{(l)}(t^{n+v}) - S_{j,h}^{(l-1)}(t^{n+v})) / S_{j,h}^{(l)}(t^{n+v})| < \varepsilon, \tag{5.1}$$

for  $v \in \{0, \frac{1}{2}, 1\}$  and  $j \in \{1, 2\}$ , with  $l =$  iteration number and  $\varepsilon = 10^{-5}$ .

This test on the speed of propagation of the moving boundaries is more severe than a test on their position  $a_{j,h}(t)$ . The corresponding number of iterations is approximately equal to 6 in the average for  $t_m < t < t_v$  and to 12 for  $t_v < t < t_f$ .

*Remark.* Each function  $S_{j,h}(t)$  is discontinuous at the times  $t^n$  (since the functions  $(Du)_{1,h}$  and  $(Du)_{2,h}$  are discontinuous); but the discontinuities are too small to be noticeable on the curves of Fig. 10. Table I shows that the jumps of the function  $S_{1,h}(t)$  are smaller than the error tolerated in the numerical solution of the discrete equations, except at the times which correspond to the first three time steps following the appearance of the moving boundary  $\mathcal{C}_1$ . The same observation is valid for the function  $S_{2,h}(t)$ . This does not mean that the existence of discontinuities for the computed functions has no importance: the influence of the discontinuities on the stability of the method has been proved in [7] and tested in [1].

*Energy Balance*

Since the function  $F(t)$  is equal to a constant, it is trivial to integrate it exactly. Hence, the approximate solution  $u_h$  satisfies the conservation relation (2.17) exactly, according to Section 4.3. But, since  $u_h$  is not computed exactly, an error is induced. Let us check the error on the energy balance between the initial time  $t = 0$  and the final time  $t = t_f$ .

TABLE I  
Problem I. Discontinuity Jumps of the Computed Speed of the First Moving Boundary (solid-liquid Interface):  $\delta S_1^n = S_{1,h}^{n+0} - S_{1,h}^n$ , for  $\Delta t = h = 1/16$

$n$	$t^n$	$S_{1,h}^n$	$S_{1,h}^{n+0}$	$\delta S_1^n$
$n_1 + 1$	0 . 3 7 5 0	0 . 1 3 6 6 7	0 . 1 3 8 0 7	0 . 0 0 1 4 0
$n_1 + 2$	0 . 4 3 7 5	0 . 1 5 7 0 6	0 . 1 5 7 1 8	0 . 0 0 0 1 2
$n_1 + 3$	0 . 5 0 0 0	0 . 1 6 2 4 3	0 . 1 6 2 4 4	0 . 0 0 0 0 1
82	5 . 0 0 0 0	0 . 0 8 3 2 7 3	0 . 0 8 3 2 7 4	0 . 0 0 0 0 0 1

*Note.* The index  $n_1 = 6$  corresponds to the time of appearance  $t_m$ .

TABLE II

Problem 1. Convergence of the Computed Values of  $t_m, t_r, t_f$  and  $a_2(t_f)$  for  $\Delta t/h = 1$ 

$h$	$t_m$			$t_r$			$t_f$			$a_2(t_f)$														
1/4	0	3	6	1	5	0	1	6	3	0	3	4	9	7	5	4	6	4	0	7	1	6	4	9
1/8	0	3	2	8	9	7	1	6	3	6	1	1	9	4	0	2	1	0	0	7	3	2	9	7
1/16	0	3	2	7	6	7	1	6	3	4	4	6	9	3	8	7	1	9	0	7	3	3	6	7
1/32	0	3	2	7	6	8	1	6	3	4	3	9	9	3	8	7	0	8	0	7	3	3	6	8

The computed values of the terms of the conservation relation (2.20) are equal to

$$\begin{aligned}
 E_1 &= 7055.081, & E_2 &= 4345.672, & E_3 &= 2160, \\
 E_4 &= 9907.216, & E_5 &= 0, & E_6 &= 23,468.03.
 \end{aligned}$$

Hence,

$$\begin{aligned}
 E &= E_1 + E_2 + E_3 + E_4 + E_5 = 23,467.97, \\
 E_6 - E &= 0.06, \\
 (E_6 - E)/E_6 &\sim 3 \times 10^{-6}.
 \end{aligned}$$

The relative error on the energy balance is of the same order as the error tolerated in the numerical solution of the discrete problem (parameter  $\varepsilon$  of (5.1)).

### Convergence and Accuracy

Table II gives the computed values of  $t_m, t_r, t_f$  and  $a_2(t_f)$  for decreasing values of  $h$  and  $\Delta t/h = 1$ . It shows that, for  $h = 1/16$ , the relative error on these values is inferior to  $10^{-4}$ . The corresponding computation time is equal to 117 sec on a CDC 7600 computer.

Let us note that it has been impossible to compute the order of accuracy of the method as in [1], because the regularity of the convergence is perturbed by

- (i) the discontinuous variation of the number of finite elements,
- (ii) the irregular variation of the time steps  $\Delta t^n$  at the times of appearance and disappearance of the phases.

Yet, the convergence seems to be as fast as in [1] (third order accuracy).

Figure 11 represents the set of all finite elements for  $h = 1/16$  and  $\Delta t = 1/4$ .

### Starting Motion of the Free Boundaries

According to the remark of Section 2.2, we expect the free boundaries to start with an initial speed equal to zero. This property does not appear clearly on the curves of Fig. 10. For a more thorough study of the motion of the free boundaries just after their appearance, we have made computations with a smaller time step: for each

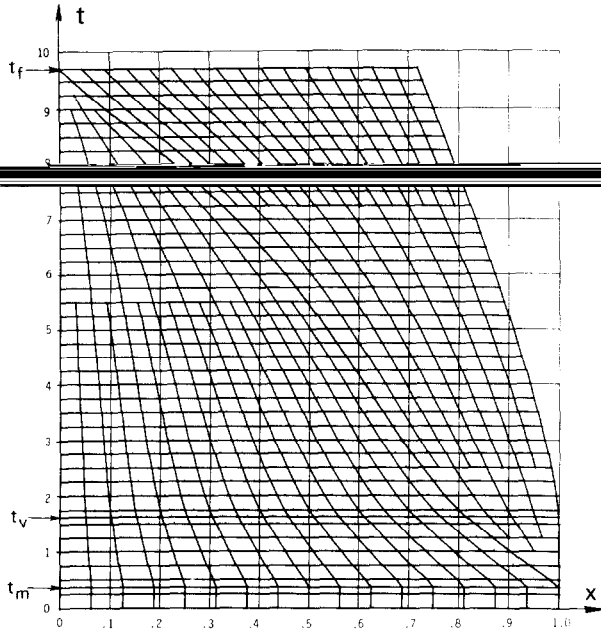


FIG. 11. Problem 1. The set of all finite elements for  $h = 1/16$  and  $\Delta t = 1/4$ .

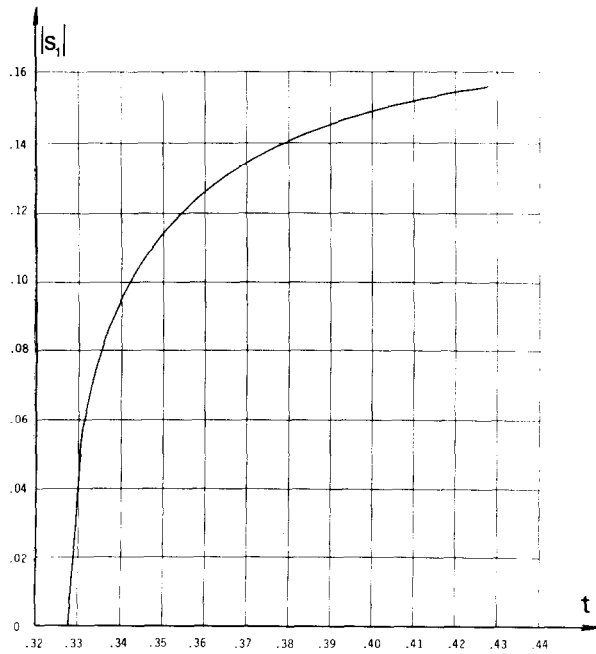


FIG. 12. Problem 1. Speed of the solid-liquid interface,  $S_1 = da_1/dt$ , near the time of its appearance  $t_m = 0.32768$ , computed with  $h = 1/16$ ,  $\Delta t = h/10$ .

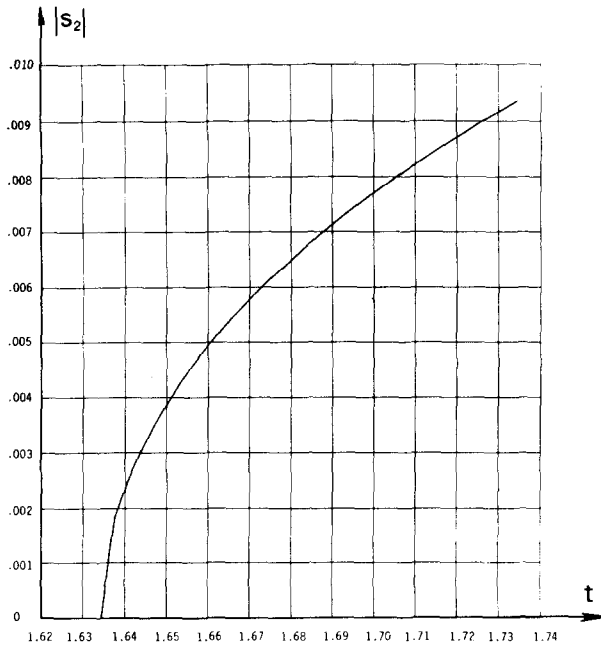


FIG. 13. Problem 1. Speed of the liquid-vapor interface,  $S_2 = da_2/dt$ , near the time of its appearance  $t_r = 1.6343$ , computed with  $h = 1/16$ ,  $\Delta t = h/10$ .

boundary we have taken  $\Delta t = h = 1/16$  until the time  $t_j$  at which it appears, then  $\Delta t = h/10$  for  $t > t_j$ . The results are represented on Figs. 12 and 13.

### 5.2. Problem 2

This problem is the same as Problem 1 except for the material which is characterized by the following values of the constants:

$$c_1 = c_2 = 1.041\rho \text{ with } \rho = 2.77, \quad K_1 = 1.73, \quad K_2 = 0.865,$$

$$C_m = 400\rho, \quad C_v = 10,700\rho, \quad u_m = 638, \quad u_v = 2480.$$

The curves of Figs. 14, 15 and 16 illustrate the results obtained for  $\Delta t = h = 1/16$ . They show that the temperature on the right boundary  $x = 1$  has not reached the vaporization temperature  $u_v$  at the final time  $t_f$  at which the solid disappears.

#### Energy Balance

We have:

$$E_1 = 1761.861, \quad E_2 = 1943.151, \quad E_3 = 1108,$$

$$E_4 = 0, \quad E_5 = 0, \quad E_6 = 4813.049,$$

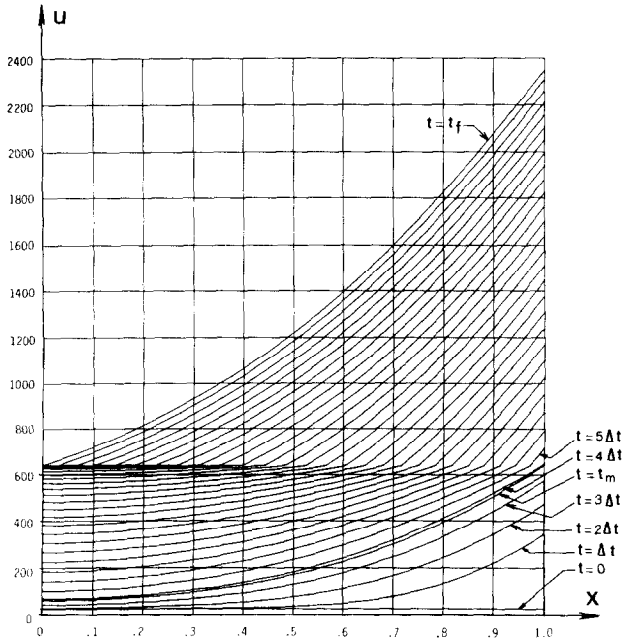


FIG. 14. Problem 2. The temperature  $u(x, t)$  at all time steps (computed with  $\Delta t = h = 1/16$ ).

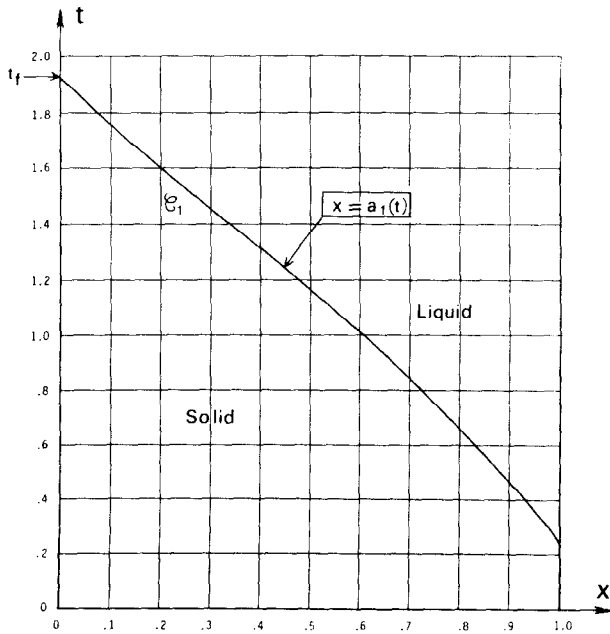


FIG. 15. Problem 2. Appearance, movement and disappearance of the free boundary ( $\Delta t = h = 1/16$ ).

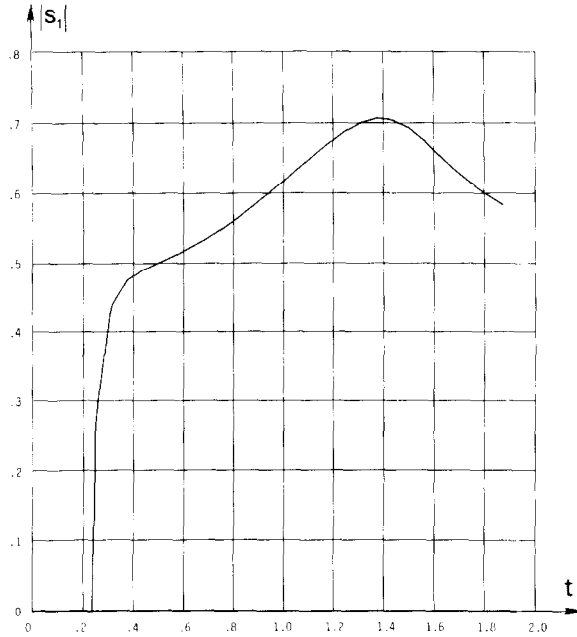


FIG. 16. Problem 2. Speed of the free boundary (computed with  $\Delta t = h = 1/16$ ).

Hence,

$$E = E_1 + E_2 + E_3 + E_4 + E_5 = 4813.012,$$

$$E_6 - E = 0.037,$$

$$(E_6 - E)/E_6 \sim 7 \times 10^{-6}.$$

The relative error on the balance of energy is of the same order as the parameter  $\varepsilon$  of (5.1).

### Convergence

Table III gives the values of  $t_m$ ,  $t_f$  and the final temperature on the right boundary  $u_f = u(1, t_f)$  computed for several values of  $h$ , with  $\Delta t/h = 1/4$ . It shows that the relative error on these values is of the order of  $10^{-5}$  for  $h = 1/8$  and  $\Delta t = 1/32$ . The corresponding computation time is equal to 26 sec on a CDC 7600 computer.

*Remark.* If we take  $\Delta t/h = 1$ , the main contribution to the error comes from the time discretization. For example, we have observed that the values computed with  $\Delta x = 1/8, 1/16, 1/32$  and  $\Delta t = 1/16$  are almost identical; but, with  $\Delta t = 1/32$  we get values which are different from the previous ones. This observation has led us to choose  $\Delta t/h = 1/4$ . This reduction of the time step was not imposed by a stability condition. It is normal to take a smaller time step in problem 2 than in problem 1

TABLE III

Problem 2. Convergence of the Computed Values of  $t_m$ ,  $t_f$  and  $u_f = u(1, t_f)$  for  $\Delta t/h = 1/4$

$h$	$t_m$				$t_f$				$u_f$										
1/4	0	.2	3	4	8	.5	0	1	.9	2	5	3	6	2	3	4	9	.1	8
1/8	0	.2	3	4	0	0	7	1	.9	2	3	8	3	2	3	4	7	.9	8
1/16	0	.2	3	4	0	0	2	1	.9	2	3	8	1	2	3	4	7	.9	6

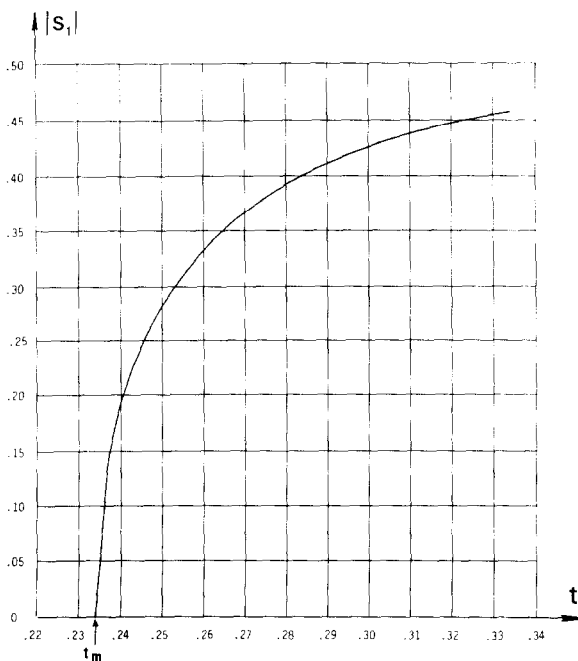


FIG. 17. Problem 2. Speed of the free boundary near the time of its appearance ( $h = 1/16$ ,  $\Delta t = h/10$ ).

since the evolution of the phenomena is faster ( $t_f = 9.3870$  in Problem 1 vs.  $t_f = 1.9238$  in Problem 2).

*Starting Motion of the Free Boundary*

Figure 17 represents the speed of the solid-liquid interface in the neighborhood of the appearance time  $t_m = 0.23400$ . It shows that the speed increases smoothly.

## CONCLUSION

In this paper, we have shown how the method of [1] can be extended in order to deal with multiphase problems involving the appearance and disappearance of phases. Other extensions are also possible, in the same way as our previous method [14] has been extended to problems involving convection, by Varôglu and Finn [17], and involving overheating of the liquid phase by internal absorption of radiation, by Gautier and Joecklé [15], and used as part of an algorithm for solving an inverse Stefan problem by Jochum [16].

## REFERENCES

1. R. BONNEROT AND P. JAMET, *J. Comput. Phys.* **32** (1979), 145–167.
2. J. R. CANNON, J. DOUGLAS, AND C. DENSON HILL, *J. Math. Mech.* **17** (1967), 21–33.
3. J. R. CANNON AND M. PRIMICERIO, *SIAM J. Math. Anal.* **4** (1973), 141–148.
4. P. CIARLET, “The Finite Element Method for Elliptic Problems,” North-Holland, Amsterdam, 1978.
5. J. DOUGLAS, T. DUPONT, AND M. F. WHEELER, *RAIRO* **2** (1974), 47–59.
6. R. M. FURZELAND, “A Survey of the Formulation and Solution of Free and Moving Boundary (Stefan) Problems,” Report TR/76, Brunel University, 1977.
7. P. JAMET, *SIAM J. Numer. Anal.* **15** (1978), 912–928.
8. P. JAMET AND R. BONNEROT, *J. Comput. Phys.* **18** (1975), 21–45.
9. J. A. NITSCHKE, in “Proceedings, Intensive Seminar on Free Boundary Problems, Pavia, 1979,” in press.
10. J. R. OCKENDON AND W. R. HODGKINS, “Moving Boundary Problems in Heat Flow and Diffusion,” Clarendon, Oxford, 1975.
11. B. SHERMAN, *J. Math. Anal. Appl.* **33** (1971), 449–466.
12. D. G. WILSON, A. D. SOLOMON, AND P. T. BOGGS, “Moving Boundary Problems,” Academic Press, New York, 1978.
13. D. G. WILSON, A. D. SOLOMON, AND J. S. TRENT, “A Bibliography on Moving Boundary Problems with Key Word Index,” Report ORNL/CSD-44, Oak Ridge National Laboratory, 1979.
14. R. BONNEROT AND P. JAMET, *J. Numer. Meth. Engrg.* **8** (1974), 811–820.
15. B. GAUTIER AND R. JOECKLÉ, in “Proceedings, Second International Conference on Lasers and Applications, Orlando, Florida, December 1979.”
16. P. JOCHUM, *Numer. Math.* **34** (1980), 411–429.
17. E. VARÔGLU AND L. FINN, *J. Comput. Phys.* **34** (1980), 371–389.